Received: 13 November 2019 | Revised: 23 December 2019 | Accepted: 23 December 2019

DOI: 10.1111/nmo.13799

ORIGINAL ARTICLE

Neurogastroenterology & Motility NGM WILEY

Ghrelin-insulin-like growth factor-1 axis is activated via autonomic neural circuits in the non-alcoholic fatty liver disease

Takuro Nagoya[1] | Kenya Kamimura[1] | Ryosuke Inoue[1] | Masayoshi Ko[1] | Takashi Owaki[1] | Yusuke Niwa[1] | Norihiro Sakai[1] | Toru Setsu[1] | Akira Sakamaki[1] | Takeshi Yokoo[1] | Hiroteru Kamimura[1] | Yuka Nakamura[2] | Masaki Ueno[2] | Shuji Terai[1]

[1]Division of Gastroenterology and Hepatology, Graduate School of Medical and Dental Sciences, Niigata University, Niigata, Japan

[2]Department of System Pathology for Neurological Disorders, Brain Research Institute, Niigata University, Niigata, Japan

Correspondence
Kenya Kamimura, Division of Gastroenterology and Hepatology, Graduate School of Medical and Dental Sciences, Niigata University, 1–757 Asahimachi–dori, Chuo–ku, Niigata, Niigata, 951-8510, Japan.
Email: kenya–k@med.niigata–u.ac.jp

Funding information
Japan Society for the Promotion of Science, Grant/Award Number: 18K19537; Gant for Interdisciplinary Joint Research Project from Brain Research Institute, Niigata University

Abstract

Background: The correlation of the growth hormone (GH) and insulin-like growth factor-1 (IGF-1) with non-alcoholic fatty liver disease (NAFLD) has been reported in epidemiological studies. However, the mechanisms of molecular and inter-organ systems that render these factors to influence on NAFLD have not been elucidated. In this study, we examined the induction of ghrelin which is the GH-releasing hormone and IGF-1, and involvement of autonomic neural circuits, in the pathogenesis of NAFLD.

Methods: The expression of gastric and hypothalamic ghrelin, neural activation in the brain, and serum IGF-1 were examined in NAFLD models of choline-deficient defined l-amino-acid diet-fed, melanocortin 4 receptor knockout mice, and partial hepatectomy mice with or without the blockades of autonomic nerves to test the contribution of neural circuits connecting the brain, liver, and stomach.

Key Results: The fatty changes in the liver increased the expression of gastric ghrelin through the autonomic pathways which sends the neural signals to the arcuate nucleus in the hypothalamus through the afferent vagal nerve which reached the pituitary gland to release GH and then stimulate the IGF-1 release from the liver. In addition, high levels of ghrelin expression in the arcuate nucleus were correlated with NAFLD progression regardless of the circuits.

Conclusions: Our study demonstrated that the fatty liver stimulates the autonomic nervous signal circuits which suppress the progression of the disease by activating the gastric ghrelin expression, the neural signal transduction in the brain, and the release of IGF-1 from the liver.

KEYWORDS

autonomic nervous system, ghrelin, IGF-1, neural circuits, non-alcoholic liver disease

Abbreviations: AAV, adeno-associated virus; CAG, hybrid construct consisting of the cytomegalovirus (CMV) enhancer fused to the chicken beta-actin promoter; CDAA, choline-deficient defined l-amino-acid diet; c-fos, proto-oncogene c-Fos; EGFP, enhanced green fluorescent protein; GH, growth hormone; IGF-1, insulin-like growth factor-1; MC4R, melanocortin 4 receptor; NS, no statistical significance; NAFLD, non-alcoholic fatty liver diseases; NASH, non-alcoholic steatohepatitis; OCT, optimal cutting temperature; PBS, phosphate-buffered saline.

1 | INTRODUCTION

Various causes of non-alcoholic steatohepatitis (NASH) and non-alcoholic fatty liver disease (NAFLD), such as metabolic syndrome, diet, genetic factors, environmental factors, and race, can be considered.[1,2] However, since multiple factors are involved, the exact cause has not been identified. Therefore, standard treatments have not been established.

Among the factors, a significantly high rate of complications of NAFLD has been observed in hypopituitarism with growth hormone (GH) deficiency, pediatric GH deficiency, and even in patients with adult GH deficiency.[3-6] In detail, NAFLD and NASH were found to be present in 70% and 21% of GH-deficient patients, respectively. This incidence is much higher than that reported in the general population (12% and 5%, respectively).[4] Interestingly, the patients with GH replacement therapy tended to have significantly improved hepatic fatty deposits and fibrosis,[4] and this effect persists for 2 years.[7] GH itself is also heavily involved in metabolic regulation and aging. After the growth period, GH hyposecretion, which is termed "somatopause", causes muscle and bone loss, visceral fat accumulation type of obesity, and fatty liver.[8] GH contributes to the secretion of insulin-like growth factor-1 (IGF-1) from the liver. Interestingly, a decrease in the concentration of IGF-1 has also been associated with the severity of hepatic inflammation and fibrosis.[9-12] In animal models of NASH and hepatic cirrhosis, IGF-1 replacement therapy was effective in reducing inflammation and fibrosis.[13,14] These therapeutic effects of GH and IGF-1 supplementation include the mechanisms of inhibition of hepatic fat synthesis,[15] inhibition of Kupffer's cell function,[16] reduction of oxidative stress in hepatocytes,[17] induction of senescence to hepatic Kupffer's cells,[13] hepatocyte proliferation,[18] and stimulation of autophagy.[19] Apart from the liver,[16] these effects were also observed in the heart, increasing the muscle mass and improving cardiac function.[20] In addition, the lower levels of serum GH and IGF-1 in the general population have been related to NAFLD.[14,21] These reports suggest that GH and IGF-1 are related to NAFLD/NASH and are essential to prevent the disease progression.

The release of GH is controlled by the GH-releasing hormone and ghrelin, which is known as an endogenous GH secretagogue.[22] Ghrelin, a 28-amino acid peptide, secreted into the blood and modified by the fatty acid octanoic acid to be an active form.[22] In addition to being mainly secreted from X/A cells, which are endocrine cells of the fundic glands of the stomach, ghrelin is also produced in the intestines, hypothalamus, and the heart. Notably, its receptors are expressed in multiple organs, such as the hypothalamus, heart, gastrointestinal tract, and pancreas.[23] Its established physiological effects are to influence on the pituitary gland to secrete GHs *via* afferent vagus nerve signals from the stomach to the solitary nucleus of the brainstem and stimulation of the arcuate nucleus *via* the signal from the solitary nucleus to promote appetite.[24] In addition, ghrelin is closely related to feeding behavior and functions as a hormone that transmits a hunger signal from the periphery to the center.[25] Hypothalamic ghrelin is one of the feeding-related peptides contributing to an increase in food intake and bodyweight.[24,26] During the initiation of meals, it increases gastric secretions during fasting, increases blood levels, and returns after eating.[25] Research using knockout (KO) mice [27] showed various phenotypes, including fatty liver, disturbed gastrointestinal motility, decreased blood pressure, and decreased circadian heart rate rhythms. These results highlighted the importance of ghrelin in maintaining biological homeostasis and metabolism.

Key Points

- The fatty liver stimulates the autonomic nervous signal circuits.
- The nervous circuits activates ghrelin-insulin-like growth factor-1 axis.
- The ghrelin-insulin-like growth factor-1 axis suppress the progression of the NAFLD.

Importantly, it has been reported that the levels of ghrelin and its function are significantly related to signal transduction *via* the autonomic nervous system.[28] Recently, it has been revealed that the autonomic nervous system is the key neural substrate that controls organ functions and mediates inter-organ signals not only in physiological but also in pathological conditions. Indeed, it regulates the status of various diseases,[29,30] the progression of cancer,[31,32] and liver regeneration after partial hepatectomy.[33] It promotes the release of serotonin from enterochromaffin cells in the small intestine *via* sympathetic nerve-mediated signal transduction from the liver to the brain.[33]

Based on these results, we hypothesized that the ghrelin and subsequent GH-IGF-1 expressions are induced through inter-organ autonomic neural connections in the NAFLD/NASH conditions and are necessary to maintain the liver homeostasis. Of note, although it is conceivable that their impairments cause disease progression, there are no studies directly showing the relationship of each event. In the present study, we evaluated the mechanism of the autonomic nervous circuits through which the ghrelin and IGF-1 axis are affected in animal models of hepatic steatosis.

2 | METHODS

2.1 | Animals

Animal experiments were approved by and conducted in full compliance with the regulations of the Institutional Animal Care and Use Committee at Niigata University, Niigata, Japan. Male C57BL/6J mice (n = 60, 8 weeks old, 25-30 g) were purchased from CLEA Japan, Inc, and melanocortin 4 receptor (MC4R) KO mice (n = 9, 8 weeks old, 25-30 g) were kindly provided from Dr Takayoshi Suganami (Tokyo Medical and Dental University and currently in Nagoya University) and Dr Yoshihiro Ogawa (Tokyo Medical and Dental University and currently in Kyushu University). Mice were housed under standard

conditions at a temperature of 20-23°C, humidity of 45%-55%, and in specific pathogen-free facilities.

2.2 | Development of animal models

The mice were divided into five groups: control, standard diet-fed mice; choline-deficient defined l-amino-acid diet (CDAA), mice fed with a CDAA containing 62 kcal% of fat, 18 kcal% of protein, and 20 kcal% of carbohydrate, purchased from Research Diets (catalog no A06071302) for 6 or 12 weeks; MC4R KO mice fed with standard diet for 4 months; and partial hepatectomy (PH). Each of the groups was divided into three groups: sham-operated group, capsaicin-treated group for which the topical application of capsaicin was utilized to deafferentate the afferent visceral nerve, and the vagus nerve blockade model for which either the afferent vagus nerve from the liver or afferent vagus nerve from the stomach was transected. The positive control of the hunger model was developed through 36 hours of fasting, followed by 1 hour of feeding. Five mice from each group were analyzed at the appropriate time points. Briefly, for PH, a midline skin incision was performed under general anesthesia, followed by removal of two-thirds of normal liver tissue as previously described.[33,34] For the selective afferent visceral nerve blockade, direct topical application of capsaicin (Wako Pure Chemical Industries, Osaka, Japan) dissolved in olive oil (50 mg/mL) was utilized to deafferentate the visceral nerve, which contains afferent sympathetic fibers from the hepatobiliary system.[33,35] This method did not show effects on the other nerves, including the vagus nerves.[33,36] For selective afferent vagus nerve blockade, transection of the hepatic branch of the vagus nerve (including >90% of the afferent vagus nerve from the liver) was performed.[33,37,38] All procedures were performed under general anesthesia using intraperitoneal injection of medetomidine hydrochloride (Nippon Zenyaku Kogyo, Fukushima, Japan) 0.3 mg/kg + midazolam (Astellas Pharma, Tokyo, Japan) 4 mg/kg + butorphanol tartrate (Meiji Seika Pharma Corporation, Tokyo, Japan) 5 mg/kg.

2.3 | Histological analysis

Tissue samples for immunohistochemical staining were collected from each group at appropriate time points after the procedures. For the PH and neural blockade groups, tissues were collected 3 days after the procedure, as previously reported.[33] Animals were deeply anesthetized with isoflurane, followed by perfusion of 4% paraformaldehyde in a transcardial manner. For the liver and stomach, tissues were fixed in 10% formalin upon tissue collection and prior to embedment in paraffin. Five different sections of the liver from each lobe and five different longitudinal vertical sections of the stomach (10 μm) were made from each of the five mice, and standard hematoxylin and eosin staining and immunohistochemistry were performed. For the brain, following the perfusion of 4% paraformaldehyde, tissues were collected, post-fixed in 4% paraformaldehyde overnight at 4°C, and embedded in paraffin. Subsequently, the tissues were carefully sectioned to expose the regions analyzed. For the expression of ghrelin, an anti-ghrelin antibody (ab57222; Abcam) at 1:200 dilution for the stomach and 1:50 dilution for the hypothalamus, the Vectastain Elite ABC mouse IgG kit (PK-6102; Vector Laboratories), and 3,3′-Diaminobenzidine chromogen tablets (Muto Pure Chemicals) were used. For the c-fos expression assay, an anti-fos monoclonal antibody (sc-166940; Santa Cruz Biotechnology), the Vectastain Elite ABC mouse IgG kit (PK-6102; Vector Laboratories), and 3,3′-Diaminobenzidine chromogen tablets (Muto Pure Chemicals) were used. Images were randomly captured from each tissue section, and quantitative analysis was performed by using the ImageJ software (version 1.6.0_20; National Institutes of Health).[39]

2.4 | Concentration of IGF-1 in the serum

Blood samples were collected prior to euthanasia, and the serum was used to analyze the levels of IGF-1 through the enzyme-linked immunosorbent assay (ELISA) using a mouse IGF-1 ELISA Kit (ab100695; Abcam).

2.5 | Adeno-associated virus (AAV) injections and immunostaining to label neural projections

C57BL/6J mice (8 and 4 weeks old) were anesthetized with isoflurane. AAV1-CAG-tdTomato (2.8×10^{12} GC/mL, 0.8 μL/site; Penn vector core, Philadelphia, PA, USA) and AAV-retro-CAG-enhanced green fluorescent protein (EGFP) (9.7×10^{12} GC/mL, 1.0 μL/site, 5 μL in total; Penn vector core) [40] were injected into the nodose ganglion and the corpus of the stomach, respectively. Four weeks after the injection, the animals were transcardially perfused using 4% paraformaldehyde. The tissues were dissected, and images of the nodose ganglion, vagus nerve, and stomach were acquired by a fluorescence stereomicroscope (SZX7, DP70; Olympus, Tokyo, Japan). They were subsequently post-fixed in the same fixatives overnight, cryopreserved in 30% sucrose in phosphate-buffered saline overnight, and embedded in Tissue-Tek optimal cutting temperature compound (Sakura Finetek). Serial sections (thickness: 20 or 50 μm) were made by using a cryostat and mounted on SuperFrost Plus slides (Thermo Fisher Scientific).

For immunohistochemical staining, sections were blocked with 5% skim milk in 0.3% Triton X-100 and phosphate-buffered saline for 2 hours and subsequently incubated with the following primary antibodies overnight at 4°C: mouse anti-ghrelin (1:200; ab57222; Abcam), rabbit anti-red fluorescent protein (1:1,000; 600-401-379; Rockland), and rabbit anti-green fluorescent protein (GFP; 1:1,000; A1112; Invitrogen). After washing with 0.1% Tween 20/phosphate-buffered saline, the sections were incubated with the following secondary antibodies for 2 hours at room temperature: Alexa

Fluor 488 or 568 donkey anti-rabbit or rat IgG (1:1000; Invitrogen). The sections were counterstained with 4′,6-diamidino-2-phenylindole or red fluorescent Nissl. Images were captured using a fluorescence microscope (BX51, DP70; Olympus).

2.6 | Statistical analyses

The data of the histological analyses and concentration of IGF-1 were statistically evaluated through one-way factor repeated-measures analysis of variance, followed by Bonferroni's multiple comparison test using the GraphPad Prism 7 software (version 7.03; MDF). A *P*-value of ≤.05 denoted statistical significance.

3 | RESULTS

3.1 | Development of animal models of hepatic steatosis and the contribution of inter-organ autonomic neural connections

We used various animal models of hepatic steatosis in this study: CDAA-fed and MC4R KO mice as a NAFLD model, and PH-treated mice as a hepatic dysfunction model with volume reduction and acute fatty infiltration. To confirm the development of hepatic steatosis in the models, the percent area of fatty change was quantitatively assessed in the liver tissue (Figure 1A,B). Compared with the sham-operated standard diet-fed mice (Figure 1A,B-CNT, Sham; 4.68% ± 1.09%), CDAA-fed mice showed a time-dependent development of hepatic steatosis of 31.17% ± 1.83% and 39.66% ± 0.87% at six (Figure 1A,B-CDAA 6W) and 12 weeks (Figure 1A,B-CDAA 12W) after CDAA administration, respectively. MC4R KO mice and PH-treated mice showed relatively milder steatosis (22.90% ± 3.21% and 18.33% ± 1.45%, respectively) (Figure 1A,B-MC4R KO, PH). The results indicate the successful development of hepatic steatosis in our models.

To examine the contribution of inter-organ autonomic neural connections to the development of hepatic steatosis, we performed neural blockade experiments. For this purpose, we have visualized the neural circuits using the AAV tracers (Figure 2). We first confirmed the connections between the brain and liver by injecting td-Tomato-expressing AAV, a viral tracer, into the nodose ganglion to label afferent vagus nerves (Figure 2A). tdTomato-positive afferent autonomic nerves were observed from the liver, which project axons to the medulla oblongata (Figure 2B,C), revealing the existence of neural pathways connecting the brain and liver. Then, the liver-brain connections were blocked on the animals having hepatic steatosis, by afferent visceral nerve blockade with capsaicin or vagus nerve transection (vagotomy), and fatty change was assessed in the liver three days later. In all the groups, no changes in steatosis were observed by the neural blockades (Figure 1B). The results indicate that liver-brain neural connections do not affect the status of steatosis at this short time period.

3.2 | Expression of ghrelin in the stomach is associated with neural signals relayed from the fatty liver

To examine the effect of neural signals from the liver to gastric ghrelin in NAFLD/NASH animal models, the levels of ghrelin expression in the cells of the stomach were quantitatively analyzed by immunostaining, combined with autonomic nerve blockades at the liver (Figure 3A,B). Compared with the level of gastric ghrelin of 2.76% ± 0.68% in controls (Figure 3A,B-CNT, Sham), MC4R KO mice showed the highest level of 10.5% ± 2.75% among the groups (Figure 3A,B-MC4R KO). CDAA 6-week (6W)-treated mice, 12-week (12W)-treated mice, and PH-treated mice also mildly increased the expression levels at 4.71% ± 0.91% (Figure 3A,B-CDAA 6W), 4.63% ± 1.10% (Figure 3A,B-CDAA 12W), and 3.34% ± 1.23% (Figure 3A,B-PH), respectively.

The level of ghrelin in control mice was not changed within 3 days of either afferent visceral nerve or afferent vagal nerve blockade (vagotomy). In mice with hepatic steatosis, however, significant suppression of ghrelin elevation was observed by the blockades, especially with the afferent visceral nerve from the liver (Figure 3B). The level of ghrelin in MC4R KO mice was inhibited by approximately 70% after afferent visceral nerve and vagus nerve blockade (3.21% ± 0.51% and 3.50% ± 0.56%, respectively) ($P < .05$; Figure 3A,B-MC4R KO). CDAA 6W-treated mice also showed a 52% inhibition (2.00% ± 1.08% [$P < .05$] and 2.49% ± 0.29%, respectively; Figure 3A,B-CDAA 6W), 12W-treated mice showed a 50% inhibition (1.94% ± 0.25% [$P < .05$] and 2.78% ± 0.54%, respectively; Figure 3A,B-CDAA 12W), and PH-treated mice showed a 68% inhibition (1.05% ± 0.20% and 1.06% ± 0.11%, [$P < .05$], respectively; Figure 3A,B-PH). The results suggest that the expression of gastric ghrelin is induced and maintained by the autonomic neural signals from the steatosis liver and may not be directly affected by the signals from the fat tissue accumulated in the liver.

3.3 | The gastric ghrelin signals are relayed to the brain via afferent vagus nerves in NAFLD

We subsequently examined whether the gastric ghrelin signals were relayed to the hypothalamus through the afferent nerves and solitary nucleus in the brainstem in the hepatic steatosis models. We first confirmed the anatomical connection between the stomach and the brain by injecting with tdTomato-expressing AAV into the nodose ganglion. A number of tdTomato-expressing sensory vagus fibers were observed in the mucosa of the stomach (Figure 2A,D). Some fibers were found to innervate close to the ghrelin-expressing epithelial cells (Figure 2D), which might be the neural substrate sensing ghrelin signals. Specific connection between the stomach and brain was further examined by injecting with EGFP-expressing AAV-retro, a retrograde viral tracer, into the corpus of the stomach (Figure 2E). EGFP-labeled afferent vagus nerves from the stomach

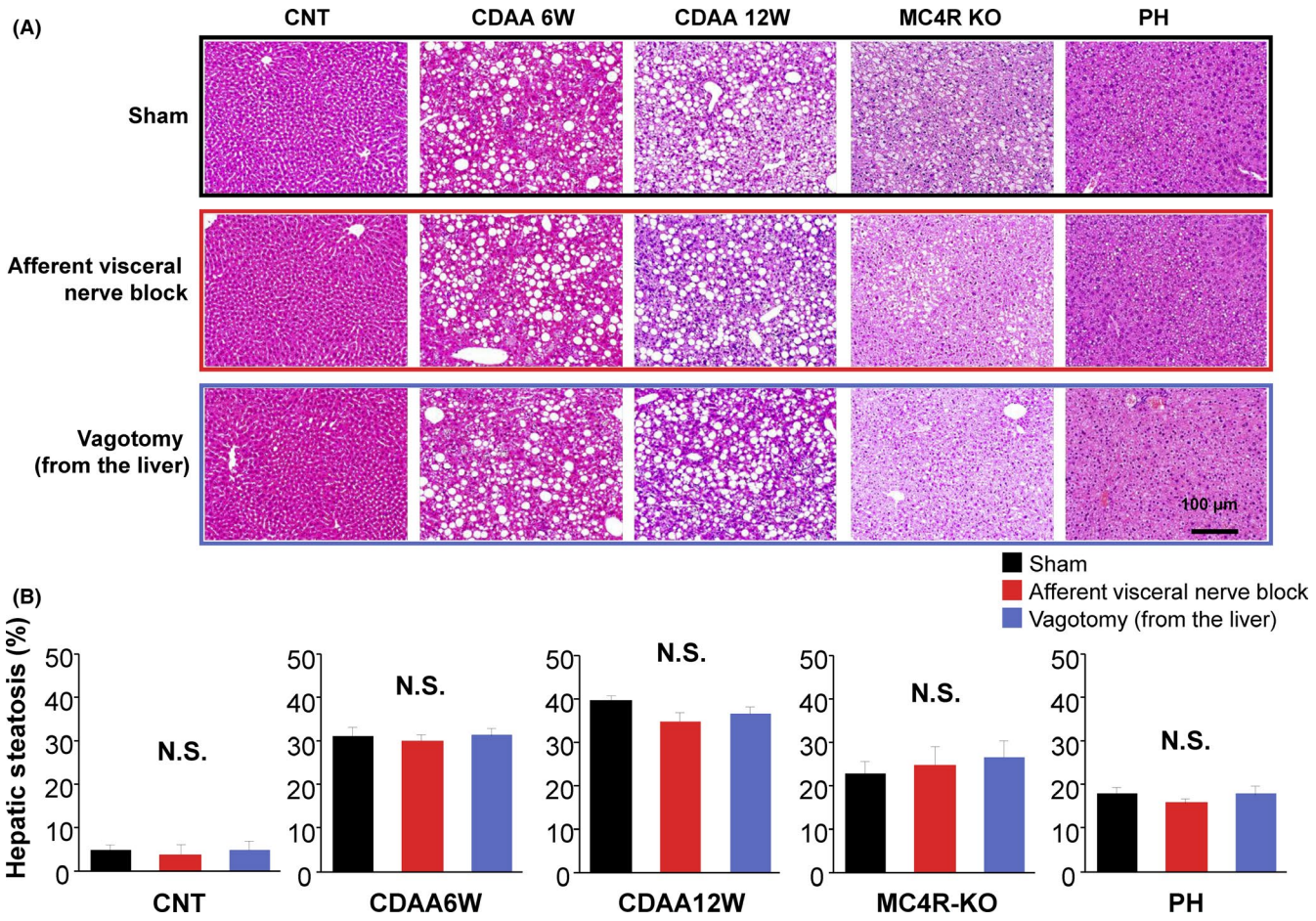

FIGURE 1 Development of NAFLD animal models. A, Representative images of hematoxylin and eosin staining of the livers in various NAFLD animal models (CNT, control group; CDAA 6W, CDAA administered for 6 wk; CDAA 12W, CDAA administered for 12 wk; MC4R KO, melanocortin 4 receptor knockout; PH, partial hepatectomy) with or without neural blockades of afferent nerves from the liver. Scale bar represents 100 μm. B, Five different sections from each of the five mice in all groups were quantitatively analyzed for fatty infiltration using the ImageJ software. The values represent mean ± SD. One-way ANOVA was performed, followed by Bonferroni's multiple comparison test. ANOVA, analysis of variance; NS, no statistical significance; NAFLD, non-alcoholic fatty liver disease; SD, standard deviation

were found to project specifically to the solitary nucleus in the medulla oblongata (Figure 2F,G). The signals from the stomach to the solitary nucleus would then send to the hypothalamic area including the arcuate nucleus.[24]

The level of c-fos expression in the arcuate nucleus was next quantitatively analyzed in the mice groups of hepatic steatosis to assess neural signal activation (Figure 4A,B). Firstly, c-fos level in the starvation mice was assessed as a positive control,[41] and 25.88% ± 2.65% of the cells were revealed to become positive (Figure 4A,B-CNT). Compared with the level of 6.34% ± 1.26% in controls (CNT, Sham; Figure 4A,B-CNT), MC4R KO mice showed the highest level of c-fos expression among the groups (30.79% ± 1.78%; Figure 4A,B-MC4R). CDAA 6W-treated mice, CDAA 12W-treated mice, and PH-treated mice also showed mildly higher levels of 15.85% ± 4.38%, 19.50% ± 2.49%, and 15.08% ± 2.01%, respectively (Figure 4A,B-CDAA 6W, CDAA 12W, PH). We further examined the effects of nerve blockade on hypothalamic c-fos expressions. The level of c-fos in control mice did not change within 3 days of either afferent visceral nerve or afferent vagal nerve blockade from the stomach (vagotomy). In contrast, the elevated levels of c-fos in mice with hepatic steatosis were significantly suppressed, especially after blockade of the afferent vagus nerve. The level of c-fos in MC4R KO mice was inhibited approximately by 38% after afferent vagus nerve blockade (18.85% ± 3.19% [$P < .05$] of positively stained cells; Figure 4A,B-MC4R). The c-fos levels in CDAA 6W-treated mice also showed a 30% inhibition (11.23% ± 3.35% [$P < .05$]; Figure 4A,B-CDAA 6W), while that in 12W-treated mice showed a 21% and 33% inhibition (15.45% ± 1.75% and 12.97% ± 2.09%) by afferent vagus nerve and visceral nerve blockade, respectively ($P < .05$; Figure 4A,B-CDAA 12W). These results suggest that the gastric ghrelin signals are conveyed to the brain *via* the vagus nerve to activate hypothalamic neurons in NAFLD models. In addition, we found that the signals were highly activated in the MC4R model at the same level with the starvation model (Figure 4). Therefore, the activation of fatty change in the liver-gastric ghrelin-brain axis *via* the autonomic pathways may be linked to the neural circuits related to appetite in the brain.

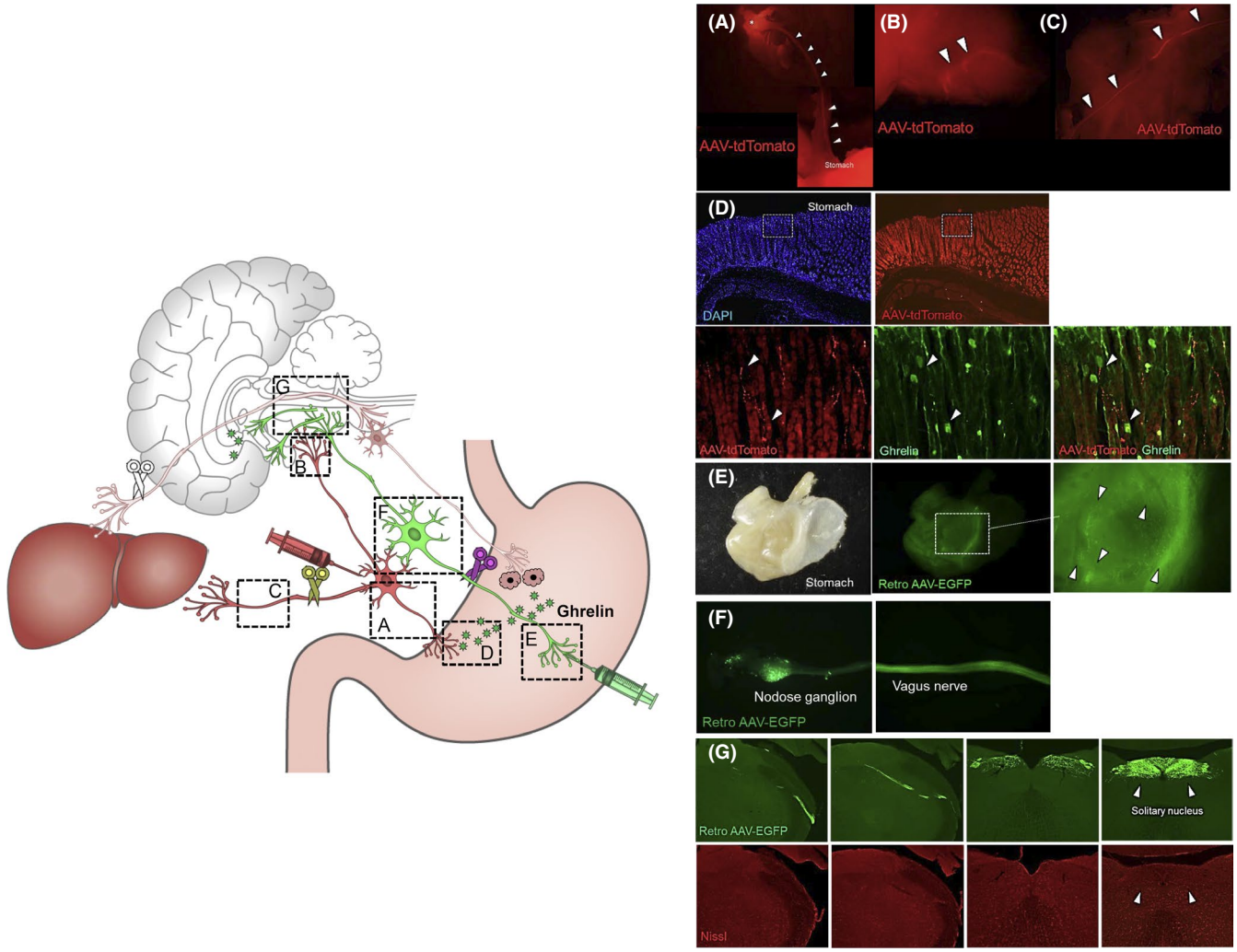

FIGURE 2 Organ and neural connections related to the pathogenesis of hepatic steatosis. A–D, AAV1-CAG-tdTomato injected into the nodose ganglion (A, asterisk; red neuron images) represents the afferent autonomic nerve from the liver (C) and stomach (D), which relays to the medulla oblongata (B) (A-D, arrowheads). E-G, AAV-retro-CAG-EGFP injected into the corpus of the stomach (E, arrowheads; green neuron images) specifically labeled the afferent vagus nerve from the stomach (E, F), which project axons to the solitary nucleus in the medulla oblongata (G). The solitary nucleus then conveys signals to the arcuate nucleus in the hypothalamus and pituitary gland. In the left panel of schema, white neural fibers indicate the afferent visceral nerve and efferent vagal nerve from the dorsal nucleus in the medulla. The yellow and purple scissors represent the neural blockade to the afferent vagus nerve from the liver and stomach, respectively. AAV, adeno-associated virus; CAG, hybrid construct consisting of the cytomegalovirus (CMV) enhancer fused to the chicken beta-actin promoter; EGFP, enhanced green fluorescent protein

3.4 | The activation of gastric ghrelin-IGF-1 axis is related to NAFLD

Since ghrelin is known as the GH secretagogue, and it increases the levels of GH and subsequent IGF-1 secretion from the liver,[22] we examined the amount of IGF-1 in the serum (Figure 5). Compared with the level of IGF-1 of 13.8 ± 4.5 ng/mL observed in control group (CNT, Sham), MC4R KO mice showed increase in serum IGF-1 at the highest level (21.7 ± 3.8 ng/mL). CDAA 6W-treated mice, CDAA 12W-treated mice, and PH-treated mice also showed mild increase in IGF-1 (8.9 ± 3.6 ng/mL, 13.2 ± 2.4 ng/mL, and 14.9 ± 3.1 ng/mL, respectively; Figure 5). Because the IGF-1 elevation might be induced by GH which would be stimulated via the stomach to the hypothalamic neural pathways, the effects of afferent nerve blockades from the stomach onto IGF-1 expressions were then examined. The concentration of IGF-1 in control mice did not show changes within 3 days after either afferent visceral nerve or afferent vagal nerve blockade from the stomach. However, after the blockades, increases of IGF-1 levels in mice with hepatic steatosis were significantly suppressed, especially after the blockade of afferent vagus nerve. The IGF-1 level in the serum of MC4R KO mice was inhibited by approximately 54% after the nerve blockade (10.0 ± 3.8 ng/mL [$P < .05$]). The levels in CDAA 6W-treated mice were inhibited by approximately 60% (2.9 ± 3.1 ng/mL [$P < .05$] and 3.6 ± 3.3 ng/mL, respectively), while those in 12W-treated mice were suppressed by 90% and

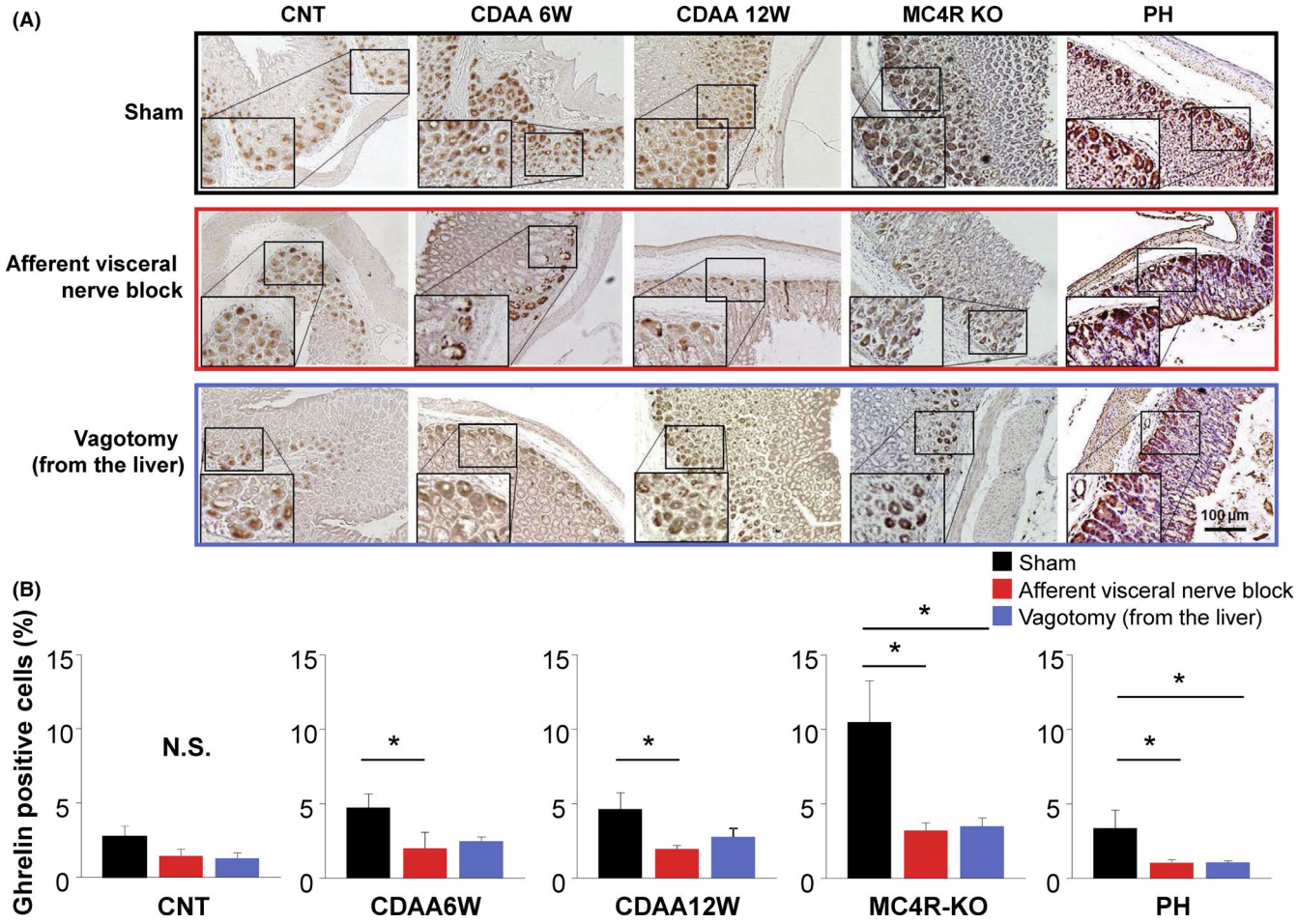

FIGURE 3 Expression of gastric ghrelin in the NAFLD and the contribution of autonomic neural pathways. A, Representative images of ghrelin expressions in the stomach in NAFLD animal models (CNT, control group; CDAA 6W, CDAA administered for 6 wk; CDAA 12W, CDAA administered for 12 wk; MC4R KO, melanocortin 4 receptor knockout; PH, partial hepatectomy) with or without neural blockade of afferent nerves from the liver. Immunostaining with an anti-ghrelin antibody. Scale bar represents 100 μm. B, Five different sections from each of the five mice in all groups were quantitatively analyzed for the ghrelin-positive cells using the ImageJ software. The values represent mean ± SD. $^{*}P < .05$. One-way ANOVA was performed, followed by Bonferroni's multiple comparison test. ANOVA, analysis of variance; NS, no statistical significance; NAFLD, non-alcoholic fatty liver disease; SD, standard deviation

59%, respectively (0.7 ± 0.6 ng/mL and 5.4 ± 3.2 ng/mL, $P < .05$; Figure 5). Notably, PH-treated mice did not show significant changes in the IGF-1 concentration, consistent with the results of c-fos activation (Figure 4B-PH). The results suggest that the level of IGF-1 in the serum is regulated by the afferent neural signals in the gastric ghrelin-brain axis that senses fatty changes in the liver.

3.5 | Increase of ghrelin in the brain is correlated with NAFLD regardless of the afferent autonomic nerves

To determine the relationship between gastric ghrelin and ghrelin in the brain, the expression level of ghrelin in the arcuate nucleus of the hypothalamus was examined in mice with hepatic steatosis (Figure 6A,B). Compared with the numbers in controls (CNT, Sham; 7.45% ± 2.03%; Figure 6A,B-CNT), MC4R KO mice increased the number of ghrelin-positive cells (9.54% ± 0.58%; Figure 6A,B-MC4R KO) at the highest level among the groups. CDAA 6W-treated mice and CDAA 12W-treated mice also mildly increased the number (5.4% ± 3.6% and 8.1% ± 3.7%, respectively; Figure 6A,B-CDAA 6W, CDAA 12W), whereas no significant increase was observed in PH-treated mice (2.0% ± 1.1%; Figure 6A,B-PH). The contribution of afferent nerve pathways was then examined by neural blocked experiments. However, significant inhibition of ghrelin expression was not observed in any group with neural blockade (Figure 6B). The results indicate that the hypothalamic ghrelin is also induced by hepatic steatosis, although it is independent of the autonomic neural circuits, which send the status of peripheral ghrelin or NAFLD of the liver to the brain. In addition, PH showed the same level of ghrelin with that of controls, suggesting that the surgical procedure in the peripheral organ has no effect on the expression of ghrelin in the hypothalamus (Figure 6).

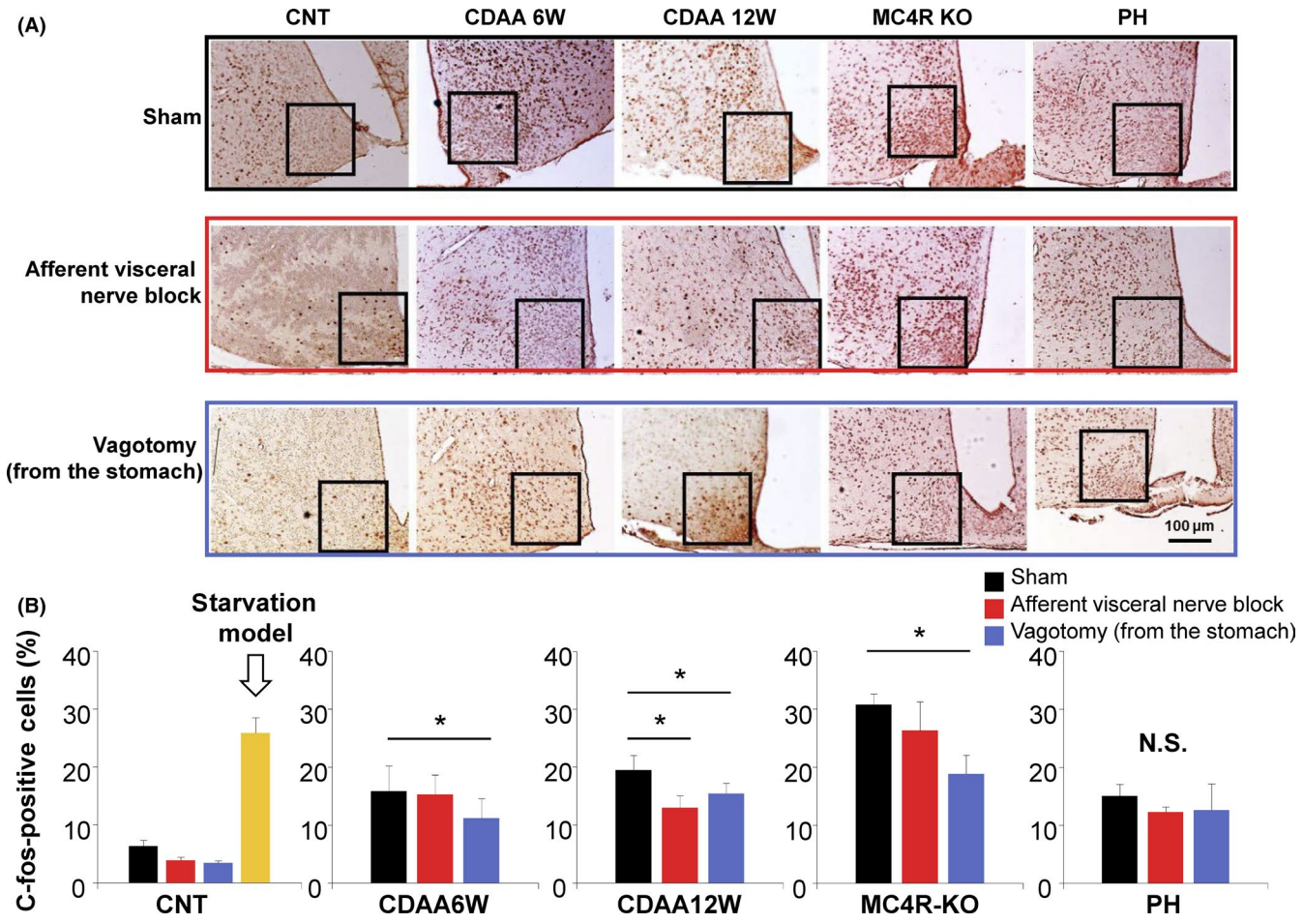

FIGURE 4 Expression of c-fos in the arcuate nucleus of hypothalamus in the NAFLD and the contribution of afferent nerve signals from the stomach. A, Representative images of c-fos expressions in the arcuate nucleus in NAFLD animal models (CNT, control group; CDAA 6W, CDAA administered for 6 wk; CDAA 12W, CDAA administered for 12 wk; MC4R KO, melanocortin 4 receptor knockout; PH, partial hepatectomy) with or without neural blockades of afferent nerves from the stomach. Immunostaining with c-fos antibody. Scale bar represents 100 μm. B, Five different sections from each of the five mice in all groups were quantitatively analyzed for the c-fos positive cells using the ImageJ software. The values represent mean ± SD (n = 15 for each group). $^{*}P < .05$. One-way ANOVA was performed, followed by Bonferroni's multiple comparison test. ANOVA, analysis of variance; NAFLD, non-alcoholic fatty liver disease; SD, standard deviation; NS, no statistical significance

4 | DISCUSSION

In this study, we demonstrated that the neural signals from the liver with steatosis contributed to the release of IGF-1 by upregulating the expression of gastric ghrelin and activating the neural signal pathways to the brain. In addition, the levels of gastric ghrelin and IGF-1 in the serum are independent of ghrelin expression in the hypothalamus which was not related to the autonomic connections. These results supported our hypothesis that the autonomic nervous signals from the liver are involved in the pathogenesis of NAFLD by controlling the ghrelin-GH-IGF-1 axis. Ghrelin in the hypothalamus in these diseased animals may contribute to obesity, appetite, and the development of steatohepatitis *via* different biological pathways.

The autonomic neural signals from the pathological hepatic status have been demonstrated to increase the number of beta cells in the pancreas to maintain the level of blood glucose [29,30] and enterochromaffin cells of small intestine to release serotonin after partial hepatectomy.[33] These studies demonstrated that the afferent visceral nerve from the liver to the brain and efferent vagus nerve to the pancreas and small intestine contributed to maintain the homeostasis of organ systems. Our results showed that during the progression of NAFLD to NASH, steatosis tissue in the liver may induce activation of efferent vagus nerve through the afferent visceral nerve and release of gastric ghrelin (Figures 1 and 3). The increase of ghrelin further activated neural signals relayed from the stomach to the brain *via* the afferent vagus nerve to the solitary nucleus (Figures 4 and 5). Based on the fact that GH deficiency is related to the occurrence of NAFLD/NASH, patients with progressed NASH showed decreased levels of GH [3-6] and IGF-1.[9-11] The replacement of GH and IGF-1 showed recovery of the liver damage.[4,7,13,14] Thus, the damaged liver may attempt to stimulate the ghrelin-IGF-1 axis through the autonomic neural circuits to maintain the biological homeostasis of the liver. Impairment of the neuronal signal transduction may be involved in the part of "multiple-hits" in the pathogenesis of NASH.

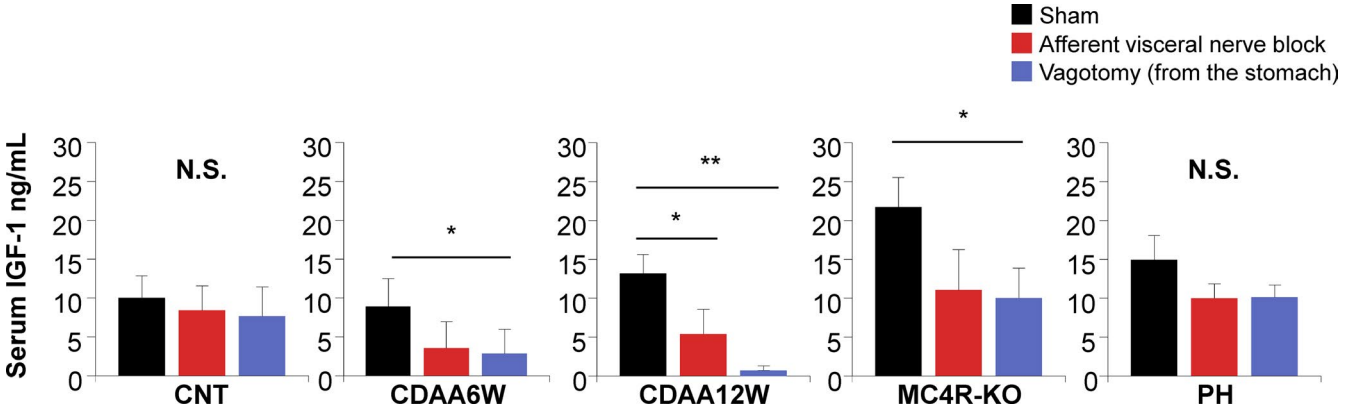

FIGURE 5 Concentration of IGF-1 in the serum in the NAFLD and its contribution of afferent autonomic nerves. A, Serum IGF-1 concentration in NAFLD animal models (CNT, control group; CDAA 6W, CDAA administered for 6 wk; CDAA 12W, CDAA administered for 12 wk; MC4R KO, melanocortin 4 receptor knockout; PH, partial hepatectomy) with or without neural blockades of afferent nerves from the stomach. IGF-1 levels were determined by ELISA. The values represent mean ± SD (n = 5 for each group). $^{*}P < .05$, $^{**}P < .01$. One-way ANOVA followed by Bonferroni's multiple comparison test. ANOVA, analysis of variance; ELISA, enzyme-linked immunosorbent assay; IGF-1, insulin-like growth factor-1; NAFLD, non-alcoholic fatty liver disease; NS, no statistical significance; SD, standard deviation

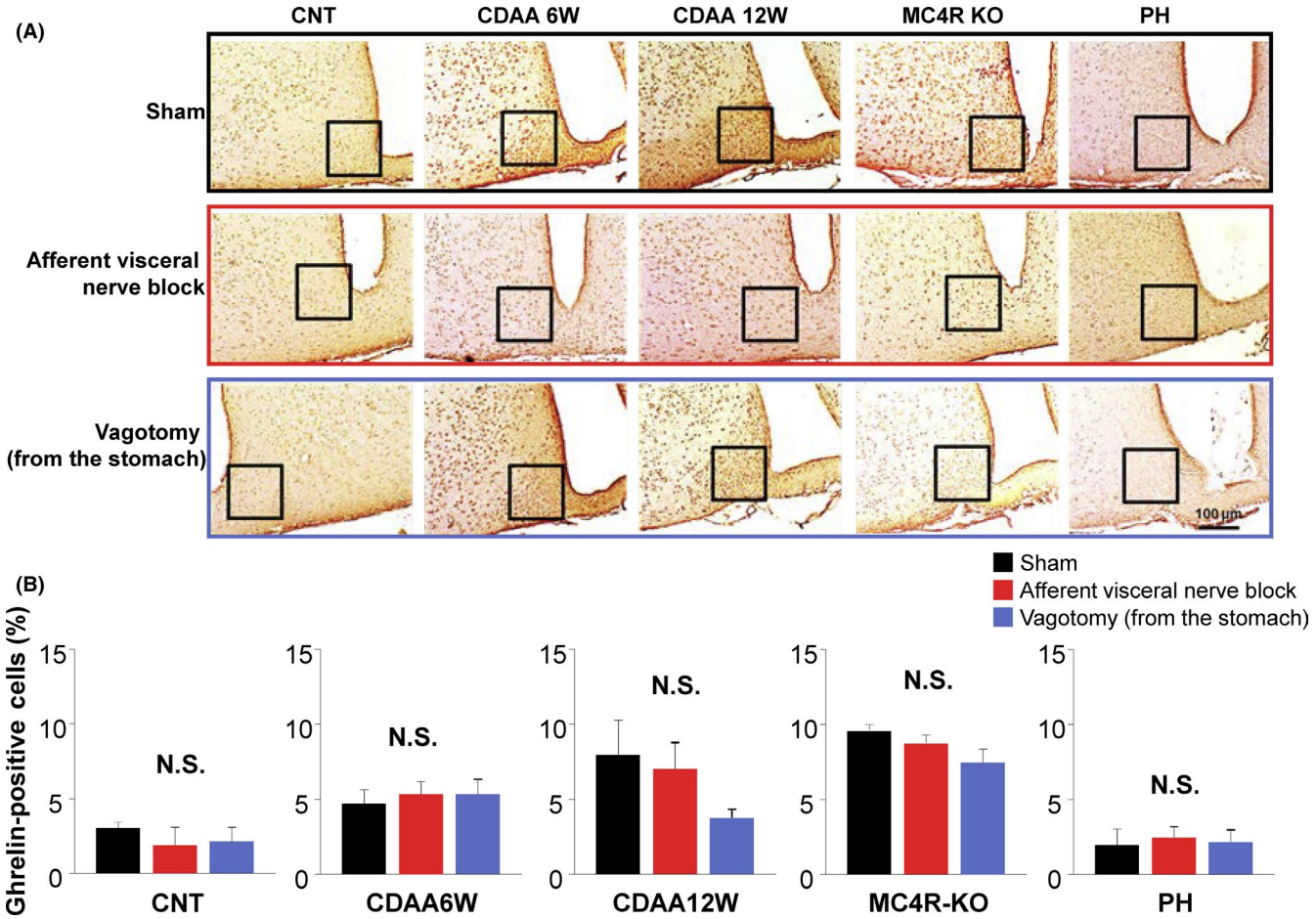

FIGURE 6 Expression of hypothalamic ghrelin in the NAFLD and its contribution of afferent autonomic nerves. A, Representative images of ghrelin expressions in the arcuate nucleus of the hypothalamus in NAFLD animal models (CNT, control group; CDAA 6W, CDAA administered for 6 wk; CDAA 12W, CDAA administered for 12 wk; MC4R KO, melanocortin 4 receptor knockout; PH, partial hepatectomy) with or without neural blockades of afferent nerves from the stomach. Immunostaining with anti-ghrelin antibody. Scale bar represents 100 μm. B, Five different sections obtained from five mice in each group were quantitatively analyzed for the ghrelin-positive cells using the ImageJ software. The values represent mean ± SD (n = 5 for each group). One-way ANOVA was performed, followed by Bonferroni's multiple comparison test. ANOVA, analysis of variance; NS, no statistical significance; NAFLD, non-alcoholic fatty liver disease; SD, standard deviation

In addition, central ghrelin is known to activate neuropeptide Y/agouti-related protein-producing neurons in the arcuate nucleus of the hypothalamus 42 and inhibits the release of anti-feeding peptides (alpha-melanocyte-stimulating hormone, a ligand for MC4R) by inhibiting arcuate nucleus proopiomelanocortin neurons.[43] Indeed, the suppression of ghrelin receptor in the brain has been reported to mitigate diet-induced obesity.[44] Although it is clear that the ghrelin in the brain contributes to an increase in food intake and bodyweight, it has also been noted that in this condition, no elevation of blood biochemical factors, such as triglycerides and cholesterols, is seen.[24] Our results showing significant activation of the gastric ghrelin-IGF-1 axis in MC4R KO mice (Figures 3-5) with high levels of hypothalamic ghrelin without changes following neural blockades (Figure 6) support the hypothesis that the impairment of central appetite control is essential in NASH pathology, whereas the activation of gastric ghrelin-brain axis is necessary to maintain biological homeostasis. The absence of increases of c-fos-positive neurons in the arcuate nucleus, IGF-1 release, and hypothalamic ghrelin in the PH group are also consistent with this hypothesis (Figures 4 and 6). Notably, the neural signal transduction from the steatosis changes in the liver with PH is not related to the appetite activated by the cerebral hormones and leads the signal to the small intestine to increase the level of serotonin.[33,45] This may also be related to the reduction of intrahepatic nerve components after the hepatic resection.

This study was characterized by some limitations. Firstly, the measurement of serum GH was difficult due to the circadian variation, although our results indicated the potential changes of its concentration in the NAFLD and NASH. Secondly, the time-dependent changes in the levels of gastric ghrelin and IGF-1 should be assessed since it is assumed that the decrease of IGF-1 as a "next hit" may be related to disease progression from NAFLD to NASH and NASH-related liver cirrhosis. Future directions should include testing the concentration of IGF-1 in a time-dependent manner to determine whether it can be used as a marker of the disease stage and as the next therapeutic option for NAFLD/NASH.

In conclusion, the present study demonstrated the relationship between NAFLD/NASH and the ghrelin-IGF-1 axis through the autonomic nervous system to maintain organ homeostasis. The signal information of the liver damage caused by fatty infiltration is sent to the brain and stomach *via* the autonomic nerve connections and increases the release of ghrelin and IGF-1. These inter-organ signals might be induced to retard the progression of NAFLD.

ACKNOWLEDGMENTS

The authors would like to thank Takao Tsuchida in the Division of Gastroenterology and Hepatology at the Niigata University for his excellent assistance in the histological analyses. The authors would also like to thank Nobuyoshi Fujisawa, Yoshitaka Maeda, Kanako Oda, Toshikuni Sasaoka, and all staff members at the Division of Laboratory Animal Resources in Niigata University. They also thank Enago for the critical reading of the manuscript and English language review. The authors declare that they have no conflict of interest. The research in the authors' laboratories has been supported in part by a Grant-in-Aid for Scientific Research from the Japanese Society for the Promotion of Sciences 18K19537 to Terai S and Kamimura K and by a grant for Interdisciplinary Joint Research Project from Brain Research Institute, Niigata University to Terai S, Kamimura K, and Ueno M.

CONFLICT OF INTEREST

The authors declare that they have no conflict of interest.

AUTHOR CONTRIBUTIONS

TN, KK, RI, MK, TO, YN, NS, TS, AS, TY, HK, YN, MU, and ST contributed to the study conception and design. TN, KK, RI, MK, TO, YN, NS, TS, AS, TY, HK, YN, and MU analyzed the study and involved in material preparation and data collection. TN, KK, and ST wrote the first draft of the manuscript, and all authors commented on previous versions of the manuscript. All authors read and approved the final manuscript.

ORCID

Kenya Kamimura https://orcid.org/0000-0001-7182-4400

REFERENCES

1. Drescher HK, Weiskirchen S, Weiskirchen R. Current status in testing for nonalcoholic fatty liver disease (NAFLD) and nonalcoholic steatohepatitis (NASH). *Cells*. 2019;8:854.
2. Nobili V, Alisi A, Valenti L, Miele L, Feldstein AE, Alkhouri N. NAFLD in children: new genes, new diagnostic modalities and new drugs. *Nat Rev Gastroenterol Hepatol*. 2019;16:517-530.
3. Takahashi Y, Iida K, Takahashi K, et al. Growth hormone reverses nonalcoholic steatohepatitis in a patient with adult growth hormone deficiency. *Gastroenterology*. 2007;132:938-943.
4. Nishizawa H, Iguchi G, Murawaki A, et al. Nonalcoholic fatty liver disease in adult hypopituitary patients with GH deficiency and the impact of GH replacement therapy. *Eur J Endocrinol*. 2012;167:67-74.
5. Ichikawa T, Hamasaki K, Ishikawa H, Ejima E, Eguchi K, Nakao K. Non-alcoholic steatohepatitis and hepatic steatosis in patients with adult onset growth hormone deficiency. *Gut*. 2003;52:914.
6. Adams LA, Feldstein A, Lindor KD, Angulo P. Nonalcoholic fatty liver disease among patients with hypothalamic and pituitary dysfunction. *Hepatology*. 2004;39:909-914.
7. Matsumoto R, Fukuoka H, Iguchi G, et al. Long-term effects of growth hormone replacement therapy on liver function in adult patients with growth hormone deficiency. *Growth Horm IGF Res*. 2014;24:174-179.
8. Cattini PA, Bock ME, Jin Y, Zanghi JA, Vakili H. A useful model to compare human and mouse growth hormone gene chromosomal structure, expression and regulation, and immune tolerance of human growth hormone analogues. *Growth Horm IGF Res*. 2018;42–43:58-65.
9. Arturi F, Succurro E, Procopio C, et al. Nonalcoholic fatty liver disease is associated with low circulating levels of insulin-like growth factor-I. *J Clin Endocrinol Metab*. 2011;96:E1640-1644.
10. Fusco A, Miele L, D'Uonnolo A, et al. Nonalcoholic fatty liver disease is associated with increased GHBP and reduced GH/IGF-I levels. *Clin Endocrinol (Oxf)*. 2012;77:531-536.
11. Sumida Y, Yonei Y, Tanaka S, et al. Lower levels of insulin-like growth factor-1 standard deviation score are associated with

histological severity of non-alcoholic fatty liver disease. *Hepatol Res*. 2015;45:771-781.
12. Yao Y, Miao X, Zhu D, et al. Insulin-like growth factor-1 and non-alcoholic fatty liver disease: a systemic review and meta-analysis. *Endocrine*. 2019;65:227-237.
13. Nishizawa H, Iguchi G, Fukuoka H, et al. IGF-I induces senescence of hepatic stellate cells and limits fibrosis in a p53-dependent manner. *Sci Rep*. 2016;6:34605.
14. Sobrevals L, Rodriguez C, Romero-Trevejo JL, et al. Insulin-like growth factor I gene transfer to cirrhotic liver induces fibrolysis and reduces fibrogenesis leading to cirrhosis reversion in rats. *Hepatology*. 2010;51:912-921.
15. Cordoba-Chacon J, Majumdar N, List EO, et al. Growth hormone inhibits hepatic de novo lipogenesis in adult mice. *Diabetes*. 2015;64:3093-3103.
16. Takahashi Y. Essential roles of growth hormone (GH) and insulin-like growth factor-I (IGF-I) in the liver. *Endocr J*. 2012;59:955-962.
17. Nishizawa H, Takahashi M, Fukuoka H, Iguchi G, Kitazawa R, Takahashi Y. GH-independent IGF-I action is essential to prevent the development of nonalcoholic steatohepatitis in a GH-deficient rat model. *Biochem Biophys Res Commun*. 2012;423:295-300.
18. Wang Q, Zheng M, Yin Y, Zhang W. Ghrelin Stimulates hepatocyte proliferation via regulating cell cycle through GSK3beta/beta-catenin signaling pathway. *Cell Physiol Biochem*. 2018;50:1698-1710.
19. Fang F, Shi X, Brown MS, Goldstein JL, Liang G. Growth hormone acts on liver to stimulate autophagy, support glucose production, and preserve blood glucose in chronically starved mice. *Proc Natl Acad Sci USA*. 2019;116:7449-7454.
20. Nagaya N, Moriya J, Yasumura Y, et al. Effects of ghrelin administration on left ventricular function, exercise capacity, and muscle wasting in patients with chronic heart failure. *Circulation*. 2004;110:3674-3679.
21. Lonardo A, Loria P, Leonardi F, Ganazzi D, Carulli N. Growth hormone plasma levels in nonalcoholic fatty liver disease. *Am J Gastroenterol*. 2002;97:1071-1072.
22. Kojima M, Hosoda H, Date Y, Nakazato M, Matsuo H, Kangawa K. Ghrelin is a growth-hormone-releasing acylated peptide from stomach. *Nature*. 1999;402:656-660.
23. Smith RG, Van der Ploeg LHT, Howard AD, et al. Peptidomimetic regulation of growth hormone secretion. *Endocr Rev*. 1997;18:621-645.
24. Nakazato M, Murakami N, Date Y, et al. A role for ghrelin in the central regulation of feeding. *Nature*. 2001;409:194-198.
25. Wren AM, Seal LJ, Cohen MA, et al. Ghrelin enhances appetite and increases food intake in humans. *J Clin Endocrinol Metab*. 2001;86:5992.
26. Cabral A, Lopez Soto EJ, Epelbaum J, Perello M. Is ghrelin synthesized in the central nervous system? *Int J Mol Sci*. 2017;18:E638.
27. Sun LY, Bartke A. Tissue-specific GHR knockout mice: metabolic phenotypes. *Front Endocrinol (Lausanne)*. 2014;5:243.
28. Okada T, Waise TMZ, Toshinai K, Mita Y, Sakoda H, Nakazato M. Analysis of peripheral ghrelin signaling via the vagus nerve in ghrelin receptor-restored GHSR-null mice. *Neurosci Lett*. 2018;681:50-55.
29. Imai J, Katagiri H, Yamada T, et al. Regulation of pancreatic beta cell mass by neuronal signals from the liver. *Science*. 2008;322:1250-1254.
30. Moreau F, Seyfritz E, Toti F, et al. Early effects of liver regeneration on endocrine pancreas: in vivo change in islet morphology and in vitro assessment of systemic effects on beta-cell function and viability in the rat model of two-thirds hepatectomy. *Horm Metab Res*. 2014;46:921-926.
31. Hayakawa Y, Sakitani K, Konishi M, et al. Nerve growth factor promotes gastric tumorigenesis through aberrant cholinergic signaling. *Cancer Cell*. 2017;31:21-34.
32. Kamiya A, Hayama Y, Kato S, et al. Genetic manipulation of autonomic nerve fiber innervation and activity and its effect on breast cancer progression. *Nat Neurosci*. 2019;22:1289-1305.
33. Inoue R, Kamimura K, Nagoya T, et al. Effect of a neural relay on liver regeneration in mice: activation of serotonin release from the gastrointestinal tract. *FEBS Open Bio*. 2018;8:449-460.
34. Higgins GM, Anderson RM. Experimental pathology of liver. I. Restoration of liver of white rat following partial surgical removal. *Arch Pathol*. 1931;12:186-202.
35. Berthoud HR. Anatomy and function of sensory hepatic nerves. *Anat Rec A Discov Mol Cell Evol Biol*. 2004;280:827-835.
36. Anders RA, Subudhi SK, Wang J, Pfeffer K, Fu YX. Contribution of the lymphotoxin beta receptor to liver regeneration. *J Immunol*. 2005;175:1295-1300.
37. Balasubramanian S, Paulose CS. Induction of DNA synthesis in primary cultures of rat hepatocytes by serotonin: possible involvement of serotonin S2 receptor. *Hepatology*. 1998;27:62-66.
38. Tan X, Behari J, Cieply B, Michalopoulos GK, Monga SP. Conditional deletion of beta-catenin reveals its role in liver growth and regeneration. *Gastroenterology*. 2006;131:1561-1572.
39. Vrekoussis T, Chaniotis V, Navrozoglou I, et al. Image analysis of breast cancer immunohistochemistry-stained sections using ImageJ: an RGB-based model. *Anticancer Res*. 2009;29:4995-4998.
40. Tervo D, Hwang B-Y, Viswanathan S, et al. A designer AAV variant permits efficient retrograde access to projection neurons. *Neuron*. 2016;92:372-382.
41. Gallardo CM, Hsu CT, Gunapala KM, et al. Behavioral and neural correlates of acute and scheduled hunger in C57BL/6 mice. *PLoS ONE*. 2014;9:e95990.
42. Ferrini F, Salio C, Lossi L, Merighi A. Ghrelin in central neurons. *Curr Neuropharmacol*. 2009;7:37-49.
43. Itoh M, Suganami T, Nakagawa N, et al. Melanocortin 4 receptor-deficient mice as a novel mouse model of nonalcoholic steatohepatitis. *Am J Pathol*. 2011;179:2454-2463.
44. Wu C-S, Bongmba O, Yue J, et al. Suppression of GHS-R in AgRP neurons mitigates diet-induced obesity by activating thermogenesis. *Int J Mol Sci*. 2017;18:E832.
45. Kamimura K, Inoue R, Nagoya T, et al. Autonomic nervous system network and liver regeneration. *World J Gastroenterol*. 2018;24:1616-1621.

How to cite this article: Nagoya T, Kamimura K, Inoue R, et al. Ghrelin-insulin-like growth factor-1 axis is activated via autonomic neural circuits in the non-alcoholic fatty liver disease. *Neurogastroenterol Motil*. 2020;00:e13799. https://doi.org/10.1111/nmo.13799